CORRELATIONS OF LENGTH AND VOLUME MEASUREMENTS IN MYOFIBRIL SUSPENSIONS

DAVID R. KOMINZ

From the National Institute of Arthritis and Metabolic Diseases, National Institutes of Health, Bethesda, Maryland 20014

ABSTRACT Instrumentation has been developed for the rapid electronic sizing of large numbers of myofibrils. The response of myofibrils in the presence of ATP to changes in Ca^{++} concentration was examined. Shortening of myofibrils upon addition of Ca^{++} was accompanied by an increased protein effective volume of approximately 10–40%. Whereas ATPase activation and increased turbidity of myofibrils upon addition of Ca^{++} were reversible upon subsequent addition of EGTA, the shortening and swelling were irreversible. It is proposed that the swelling may result from the breaking of hydrophobic bonds within myosin. The ATPase activity and turbidity are measures of the input, while the shortening and swelling are measures of the output of a coupled nonequilibrium process; failure of reversal of the output indicates an uncoupling under the experimental conditions.

INTRODUCTION

Volume measurements on muscle and muscle models give information about the physical processes accompanying muscle contraction. Two types of volume measurement have been employed: (*a*) Marsh found a reversible swelling of about 25% upon adding ATP[1] to muscle homogenates (1). This is a volume transfer, the transfer of water between the surrounding medium and the muscle protein. Extensive use continues to be made of such measurements (2–5). (*b*) Ernst originally discovered a small loss in volume when muscle contracts (6, 7). This is an actual volume variation which can be studied inside a closed chamber by examining volume changes (6–11), pressure changes (12, 13), or the effect of varying pressure on muscle (14, 15) and on model systems (16–18).

Marsh measured the volume transfer continuously during centrifugation (1). The usual measurement as a packed volume (2–5) entails the danger that high ATPase activity in such a small volume will deplete the ATP concentration locally, even in

[1] Abbreviations used are: ATP, adenosine triphosphate; EDTA, ethylenediaminetetraacetic acid; EGTA, ethylene glycol bis (β-aminoethyl ether)-*N*,*N*-tetraacetic acid; pATP, negative logarithm of ATP concentration.

the presence of ATP-regenerating system. Thus, the process of measurement can alter the quantity being measured. In an effort to avoid this, brief simultaneous centrifugation of samples at low speed is usually employed. An alternative procedure would be to measure the volume of myofibrils in suspension one by one, and then to analyze statistically the sample of several thousand myofibrils. In the present paper, electronic-sizing techniques have been applied to myofibril suspensions.

In contrast to previous sizing experiments performed on intact cells (19, 20), chloroplasts (21), mitochondria (22), and bacteria (23), the present experiments on myofibrils involve no limiting membrane. Since only the resistivity of the structural proteins and their tightly bound water is being measured, relatively large structures give rise to relatively small signals. However, it has been possible to measure both the length and effective protein volume distributions of myofibrils as influenced by the level of free Ca^{++} in solutions of defined ATP concentration.

Because no attempt appears to have been made previously to relate volume transfer to volume variation processes in muscle, a brief exploration of this relationship is presented. Comparison of size variations to ATPase and turbidity variations has been made, and the significance of reversibility in experimental model systems has been examined.

MATERIALS AND METHODS

Myofibrils were prepared by homogenizing minced fresh rabbit psoas muscle for 4 min in 10 volumes of 0.02 M KCl, 0.008 M Tris-maleate pH 6.85 buffer containing 0.004 M EDTA. The suspension was filtered through cheesecloth and centrifuged gently at 650 *g* for 20 min at 5°C. The supernatant was discarded and the precipitate was resuspended in the same solution and centrifuged for two more washing cycles. The precipitate was brought to a concentrated suspension with a small volume of the same solution, diluted slowly with an equal volume of ice-cold glycerol, and stored in the Deep-freeze at −20°C until used.

Signals were generated with a Celloscope Model 111 (Particle Data, Inc., Elmhurst, Ill.). They were fed into a Didac Model SA 43 (Intertechnique Instruments, Inc., Dover, N. J.), which acted as an analogue to digital converter and a multichannel analyzer. The techniques employed were similar to those used for the determination of swelling in mitochondrial suspensions by Gebicki and Hunter (22). A hollow tube is immersed in a beaker containing the particles to be examined suspended in a conducting electrolyte solution. There is an aperture in the tube 60 μ in diameter and 60 μ in length. One electrode is immersed in the suspension, and a second electrode is inside the hollow tube; a constant current is maintained between them. A suction system, utilizing a rising column of mercury which sequentially trips two relays, allows measurements to be made while exactly 0.5 ml of suspension is being sucked from the beaker through the orifice.

As each particle passes through the aperture, it causes a momentary increase in resistance, which the constant current characteristics of the instrument translate into a momentary increase in voltage. Some typical pulses obtained with human erythrocytes and with rabbit myofibrils are illustrated in Fig. 1. These are Celloscope output signals displayed on a Tektronix type RM 561A cathode ray oscilloscope (Tektronix, Inc., Beaverton, Ore.) employing type 3A1 amplifier and type 3B3 time base. Whereas the erythrocytes form a relatively homogeneous population, the myofibrils are heterogeneous with large numbers of quite small signals; in both cases the rise times vary between about 5 and 15 μsec. The amplitude of the signal is

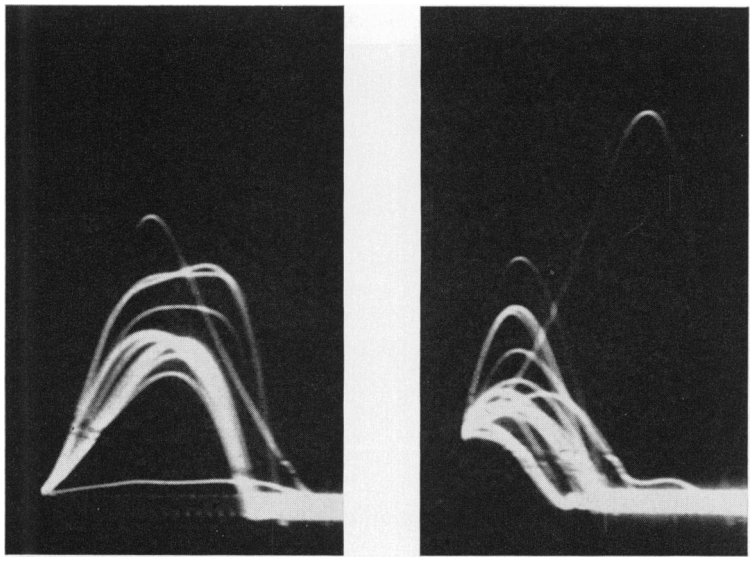

FIGURE 1 Pulse shapes produced by human erythrocytes (left) and rabbit skeletal muscle myofibrils (right). The orifice was 60 μ in diameter and 60 μ in length; Celloscope settings were 1 ma aperture current, $\times$ 6 amplification; cathode ray oscilloscope settings were 1 v/vertical division and 5 μsec/horizontal division. The suspending electrolytes were 0.15 M NaCl for erythrocytes and 0.1 M KCl, 0.5 mM Mg^{++}, 0.02 M Tris-maleate buffer pH 6.85 (stock sizing solution) for myofibrils.

dependent upon the ratio of the volume of the particle to that of the orifice. It is also dependent upon the shape and orientation of the particle; for example, compared to a rigid sphere of the same volume, a rodlike particle will have one-third less amplitude if oriented parallel and one-third more amplitude if oriented perpendicular to the orifice axis, while even greater variations in amplitude are possible with oblate ellipsoids (24).

The Celloscope output signal voltage is dependent upon the current maintained across the orifice as well as the amplification given the raw signal. If too high a product of aperture current and amplification were employed (e.g., 1.4 ma, $\times$ 48 amplification), certain circuits became saturated when large myofibrils passed through the aperture, leading to an artifically prolonged signal. This could be avoided by employing low values of aperture current and amplification (e.g. 0.12 ma, $\times$ 48 amplification; or 1 ma, $\times$ 6 amplification). Under these conditions, the linearity of the instrument is better than 1%.

Pulse height analysis was performed by the Didac. Acting as a voltmeter, it measured the voltage pulses emerging from the Celloscope many times per second, and stored each measurement in its memory for subsequent display in a statistical manner. For volume measurements, a special interface was designed and built by Mr. J. Haigh of Intertechnique Instruments, Inc. Utilizing the upper and lower thresholds of the Celloscope, the interface stretched the peak voltage of an accepted signal, gated it, and refused to accept subsequent signals for 30 μsec until the completion of processing. Less than 10% of the count recorded by the Celloscope was excluded by the interface for following too close upon an accepted signal during the processing time.

To measure particle length, the Celloscope signal was employed directly. The Didac analyzed the time interval between the triggering of a preset discriminator threshold by the leading edge and by the trailing edge of the signal, and stored the digitized information in a statistical

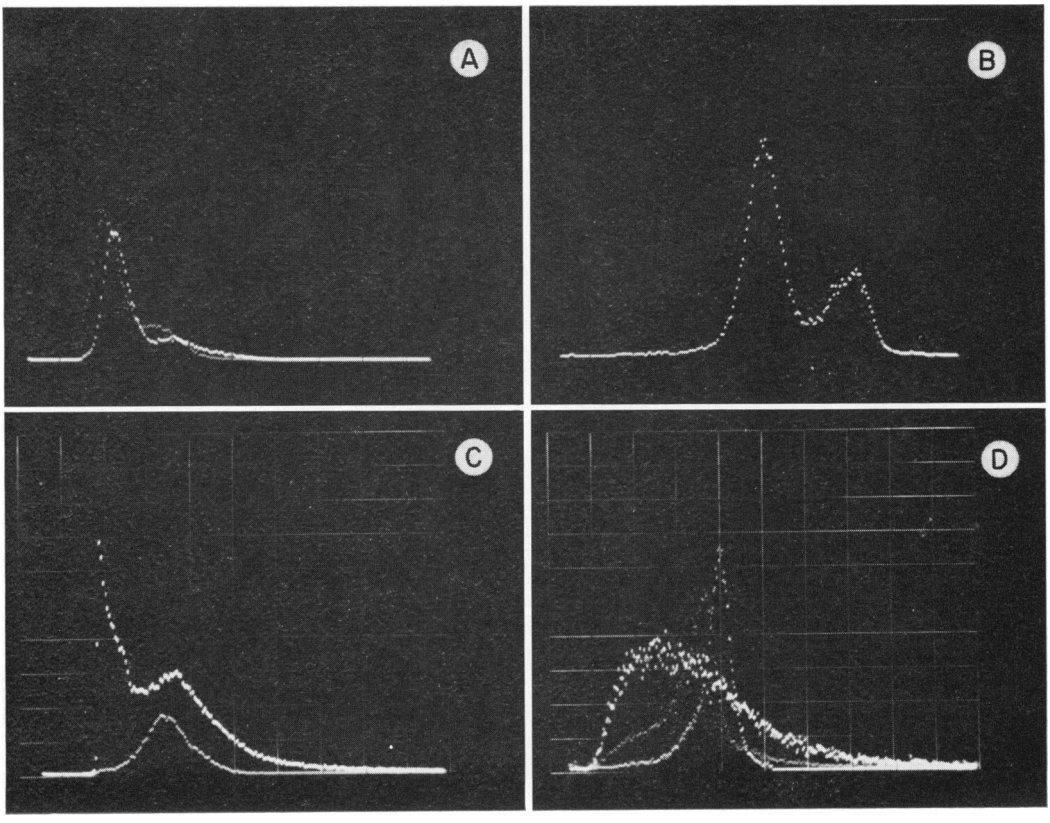

FIGURE 2 Standardization of length and volume distributions with known-sized particles. (A) Volume histogram of fresh mouse and rat erythrocytes; pale tracing was given by mouse erythrocytes (volume 50 μ^3) with the major peak at channel 38; bright tracing was given by rat erythrocytes (volume 60 μ^3) with the major peak at channel 43. (B) Length histogram of fresh mouse and rat erythrocytes; pale tracing was given by mouse erythrocytes and bright tracing was given by rat erythrocytes; both (length 6 μ) had a major peak at channel 101. (C) volume histogram of aged rat erythrocytes alone and in the presence of rabbit myofibrils. (D) length histogram of aged rat erythrocytes alone, myofibrils alone, and erythrocytes in the presence of myofibrils. In A and C there are 200 channels full scale, 20 channels per division; in B and D there are 400 channels full scale, 40 channels per division. Celloscope settings were 1 ma aperture current, $\times$ 6 amplification.

mode. It must be kept in mind that the length measurements actually are recording the duration of transit. The basic transit time is that of small spheres following the axis of the aperture. Prolonged transit times result if particles are near the aperture walls where velocity is less, or if the particles are prolate or oblate ellipsoids or flexible structures (24).

With Celloscope aperture current of 1 ma and amplifications of 6, settings routinely utilized for examination of myofibrils, standardization with known-sized particles is illustrated in Fig. 2. Fig. 2 A is the volume histogram of fresh mouse erythrocytes (volume 50 μ^3) and of fresh rat erythrocytes (volume 60 μ^3); the mouse cells have a main peak in channel 38 and a small

secondary peak near or in channel 63; the rat cells have a main peak in channel 43 and a secondary peak near or in channel 72. Extrapolation of these results with machine zero in channel 12 gives 70 μ^3 in channel 50 and 160 μ^3 in channel 100. Fig. 2 B is the length histogram of fresh mouse and rat erythrocytes (length approximately 6 μ); there is a main peak in channels 100–102 and a secondary peak in channels 145–148. Fresh human erythrocytes (length 7.5 μ) exhibited a major peak in channel 172. Extrapolation of these results with machine zero in channel 12 gives approximately 6 μ in channel 100 and 19 μ in channel 300. Figs. 2 C and D illustrate the appearance of suspensions of aged erythrocytes alone and added to suspensions of myofibrils. The myofibril volume distribution resembles that of mitochondria passing a 19 μ orifice (22); instead of a distinct peak, there is a concave curve with a sharp increase and a shoulder in the lowest channels. The length distribution forms a broad peak.

Volume measurements were stored in 200 channels of Didac memory and length measurements in 400 channels. For display and analysis, the memory was summated in 18 subgroups of 10 channels (volume) or in 19 subgroups of 20 channels (length), using the integration mode of the Didac with readout on a Model 33 Teletypwriter (Teleype Corporation, Skokie, Ill.) Since 4–5 min were required to obtain a measurement and then to integrate it, 10–12 min were required for recording the length and volume distribution after each addition to the suspension.

Because the total counts varied widely, each of the subgroups was expressed in terms of per cent of the total count. This number fraction is denoted as n_i in the case of the volume, with i representing a subgroup between 2 and 19 and $\sum n_i = 100$. The volume distributions n_i are plotted in the upper left and the differences Δn_i are plotted in the lower left of Figs. 7 and 8. The area under the difference plot is composed of an initial negative portion $\sum(-\Delta n_i)$ and a subsequent positive portion $\sum(+\Delta n_i)$, the sum of which is zero. The total volume of the myofibrils counted is $\sum n_i V_i$; to simplify the calculations, the relative V_i has been allowed to equal i. Based on the volume standardization, if $V_i = 19$ at $i = 19$, then $V_i = 1.48$ at $i = 2$; the ratio of $\sum n_i V_i$ obtained using the true value of V_i is within 1% of the ratio obtained letting $V_i = i$. The summation begins with $i = 2$ because the subgroup extending from machine zero at channel 12 to channel 20 was not measured.

Stock solution for sizing measurements was 0.1 M KCl, 0.5 mM $MgCl_2$, 0.02 M Tris-maleate buffer pH 6.85. Usually 0.1–0.2 ml myofibril suspension stored in 50% glycerol was added to 20–40 ml stock solution to obtain a count of 50,000–200,000/0.5 ml. The ATP regenerating system consisted of 0.5 mM creatine phosphate and 0.025 mg/ml creatine kinase. Usually four volume and length measurements were made on each sample: first, measurements were made in the absence of any addition; second, they were made in the presence of 10^{-5} M EGTA and 0.1–1.0 $\times$ 10^{-3} M ATP; third, 0.5–1.0 $\times$ 10^{-5} M Ca^{++} was added; and fourth, 10^{-4} M EGTA was added. Temperature was either room temperature (22–25°C) or 0°C.

The ATPase activity and turbidity were examined simultaneously in the apparatus described by Evans and Bowen (25), modified to allow temperature monitoring and control (26). The 20 ml reaction mixture contained 4–6 mg myofibrils, 0.1–0.14 M KCl, 0.5 mM $MgCl_2$, and an ATP-regenerating system of 0.05 mg *Escherichia coli* acetokinase (Boehringer Mannheim Corp., N.Y.) and 1 mM acetyl phosphate (26). The pH was brought to 7.5 and the reaction started upon addition of the ATP.

For direct length measurements, myofibrils were viewed with a Bausch & Lomb microscope (Bausch & Lomb, Inc., Rochester, N.Y.) equipped with phase optics. Photography was performed with the 4 $\times$ 5 camera and Polaroid No. 500 sheet film holder (Polaroid Corp., Cambridge, Mass.). Samples were examined in aqueous suspension or dried and stained with acid hematoxylin or gomori trichrome.

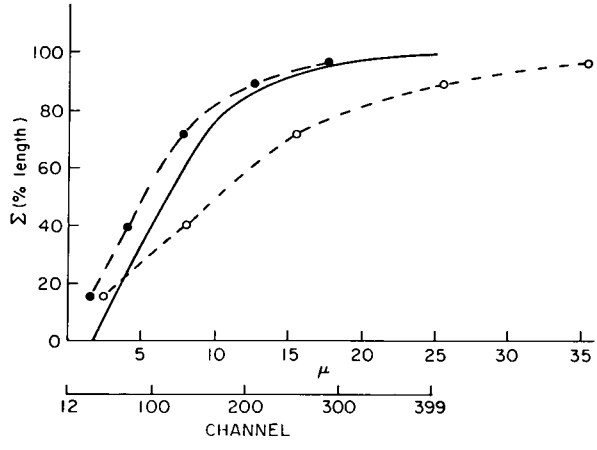

FIGURE 3 Length distribution of myofibrils from electronic sizing and from microscopic examination. ———, integrated length distribution obtained by electronic sizing in channels 21–399. O- - - -O, integrated length distribution obtained from microphotographs by measuring end-to-end distance L in μ. ●— — — —●, the same integrated length distribution plotted at $L/2$ instead of L.

RESULTS

Comparison was made between the apparent length distribution obtained from the electronic sizing (Fig. 3, solid line) and the length distribution directly measured on photomicrographs of fresh and stained myofibril preparation (Fig. 3, open circles). The end-to-end distances found in the photographs were much longer than the lengths measured electronically. Such a discrepancy would be expected if for any reason the myofibrils failed to orient on passage through the orifice. Since the Reynolds number of the orifice is 0.010, the theory of Grover and coworkers (24) indicates that halfway through the orifice, the core region will occupy 0.5–0.6 of the total orifice radius. The core region does not possess laminar flow, and consequently imposes no orientation on the myofibrillar rods. Using the usual spherical coordinates and assuming that the X axis is the direction of flow through the orifice, the projection on the X axis of randomly distributed rods can be easily calculated:

$$L_{\text{ave}} = \frac{\int_0^{\pi} d\varphi \int_{-\pi/2}^{\pi/2} L \sin \varphi \cos \theta \times \sin \varphi \, d\theta}{\int_0^{\pi} d\varphi \int_{-\pi/2}^{\pi/2} \sin \varphi \, d\theta},$$

where $0 < \varphi < \pi$, $0 < \theta < 2\pi$, and integration is limited to positive values of $X = L \sin \varphi \cos \theta$. It is found that $L_{\text{ave}} = L/2$. Values of $L/2$ are plotted as closed circles in Fig. 3; they approximate much closer the electronically determined distribution. The core region, however, occupies about 0.3 of the total cross-sectional area

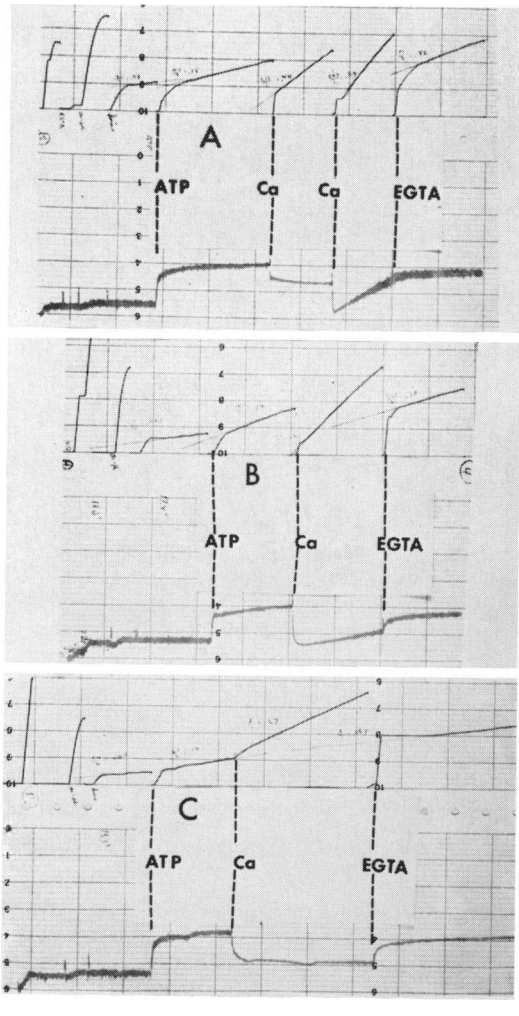

FIGURE 4 Response of myofibrillar ATPase activity and turbidity to addition of Ca^{++}, and reversibility with EGTA. The 20 ml reaction mixture contained 4 mg myofibrils, 0.14 M KCl, 0.5 mM Mg^{++}, 1 mM acetyl phosphate, 0.05 mg *E. coli* acetokinase, and either 10^{-5} M EGTA (A) or 5×10^{-6} M EGTA (B and C). At the points labeled "ATP," each solution was brought to 10^{-4} M ATP; at the points labeled "Ca," 10^{-5} M Ca^{++} was added; at the points labeled "EGTA," 10^{-4} M EGTA was added. The time scale is 3 min/division; the turbidity scale (below) is 10% transmission/major vertical division, with an upward deflection representing clearing and a downward deflection representing turbidity development. The ATPase scale (above) is 1 μmole/major vertical division; in all cases zero-order kinetics are obtained with the steepness of the slope giving a direct measure of the steady-state ATPase activity. (A) preparation 2F9, temperature 20.5°C; (B) preparation 2C9, temperature 17.4–18.3°C; (C) preparation 2C9, temperature 13.0°C.

of the orifice, and thus it alone cannot be responsible for the discrepancy in length measurements. Another factor is the flexibility of the myofibrils, apparent on microscopic examination, which could prevent or diminish orientation in the region of laminar flow.

To determine the optimum conditions for studying length and volume changes in myofibrils, ATPase and turbidity responses were first examined. As seen in all three tracings of Fig. 4, when 0.1 mM ATP was added to myofibrils in the absence of Ca^{++}, clearing occurred and the ATPase activity was low. In Fig. 4 A, a small addition of Ca^{++} raised both that turbidity and the ATPase activity; a further addition of Ca^{++} again raised the ATPase activity, but this time after a brief rise the turbidity tracing dropped off and broadened considerably. Visual and microscopic examina-

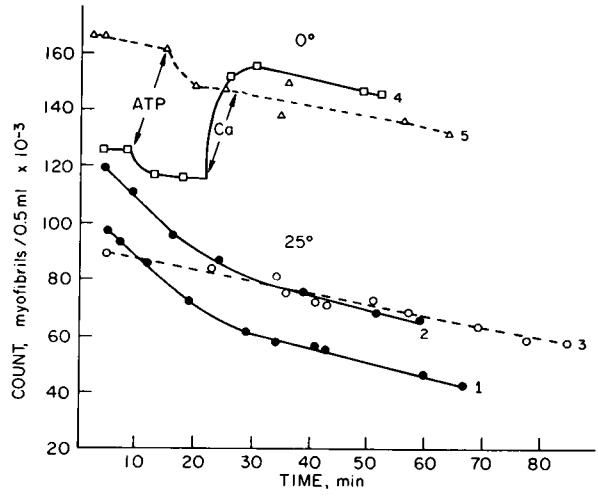

FIGURE 5 Factors influencing the time dependence of the myofibril count. Curve 1, pH 4.8-treated myofibrils in plastic beaker at 25°C. Curve 2, pH 4.8-treated myofibrils in glass beaker at 25°C. Curve 3, pH 4.8-treated myofibrils in plastic beaker prerinsed with bovine serum albumin at 25°C. Samples 1–3 were run with threshold setting 4. Curve 4, untreated myofibrils in glass beaker at 0°C, threshold setting 5. Curve 5, untreated myofibrils in glass beaker at 0°C, threshold setting 4. All samples were in stock sizing solution with ATP, Ca^{++}, and then EGTA added as described in methods. The pATP was 3.2 for samples 1–3, 3.6 for sample 4 and 3.8 for sample 5. Settings were 1 ma aperture current, × 6 magnification.

tion revealed that undesired aggregation of the fine myofibril suspension into coarse clumps had occurred. The addition of excess EGTA immediately reduced the ATPase activity and prevented the further development of aggregation, but it did not reverse either the turbidity or aggregation.

Conditions were found where it was possible to avoid this undesired aggregation and to reverse some of the turibidity. The sample in Fig. 4 B was examined at 18°C; although some aggregation occurred in this sample, part of the turibidity was reversible upon addition of EGTA. With the sample of Fig. 4 C at 13°C no clumping occurred, and both ATPase activity and turbidity were completely reversible with EGTA. (Further addition of Ca^{++} to this sample, not shown in the figure, caused aggregation to occur). Under all conditions the ATPase activity was immediately responsive to addition of EGTA, but the turbidity was only responsive to the extent that aggregation of the myofibrils had been avoided.

Will the occurence of aggregation be expected to have a deleterious effect on the electronic sizing, besides the trivial one of clogging the orifice? In principle at the same time that aggregation increases the volume of the myofibril clumps, it lowers their number so that $\sum n_i V_i$ is constant. Therefore the ratio $(\sum n_i V_i)_{\text{after}}/(\sum n_i V_i)_{\text{before}}$ should give the ratio of effective volumes for any process affecting the myofibrils, whether or not the aggregation has occurred, if all particles examined are within the

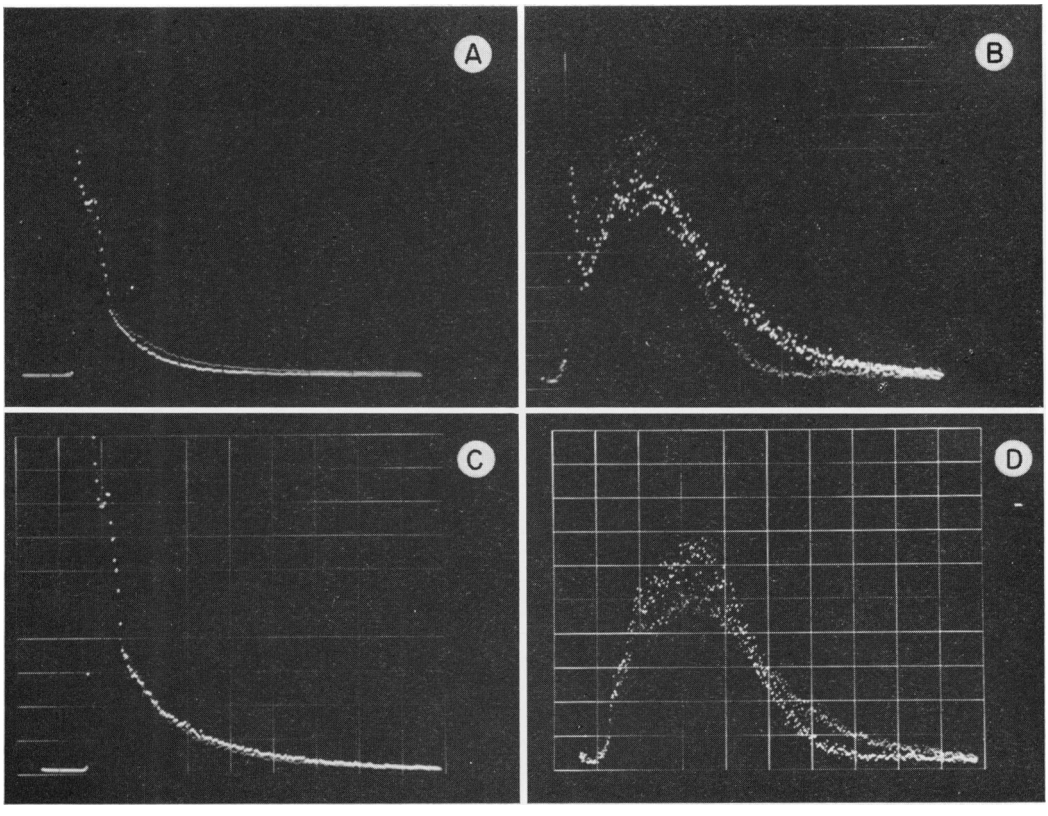

FIGURE 6 Length and volume distributions of myofibrils before and after contraction, photographed directly from Didac oscilloscope. A and C are volume histograms, covering 200 channels; B and D are length histograms, covering 400 channels. (A) Bright tracing, relaxed myofibrils at 25°C, count = 134,000; pale tracing, myofibrils contracted on adding ATP to pATP 3.8 in presence of EGTA, count = 133,000. (B) Bright tracing, relaxed myofibrils at 25°C, count = 53,000; pale tracing, myofibrils contracted on addition of ATP and Ca^{++} to pATP 3.2; count = 48,000. (C) Pale tracing, myofibrils relaxed at 0°C with ATP and EGTA present at pATP 3.8, count = 148,000; bright tracing, myofibrils contracted on addition of Ca^{++}, count = 150,000. (D) Pale tracing, myofibrils relaxed at 25°C, count = 88,000; bright tracing, myofibrils contracted after addition of ATP and Ca^{++} to pATP 3.2, count = 86,000.

thresholds for both measurements. In practice, however, excessive aggregation can create large clumps exceeding the upper threshold so that they are not counted and false low values of effective volume are obtained; if any particles were subthreshold, their aggregation would bring them within the thresholds, producing a false high value of effective volume. For accurate determinations of volume changes, aggregation clearly should be avoided. Moreover, Fig. 4 illustrates that if reversibility of Ca^{++}-induced changes is to be studied, aggregation should be avoided or kept to a minimum.

The time dependence of the myofibril count is illustrated in Fig. 5. At room temperature, there is an initial rapid drop, followed by a slower steady falloff (curves 1 and 2). It was suspected that adsorption onto the vessel walls could be lowering the count, and indeed prerinsing the beaker with a solution of bovine serum albumin eliminated the rapid initial drop (curve 3). At 0°C, different characteristics of the time dependence were observed. There was no initial rapid drop (curves 4 and 5). Upon addition of ATP in the presence of EGTA, a small drop was seen. In early studies, the subsequent addition of Ca^{++} could generate a large increase in count, such as the 35 % increase seen in curve 4. This sudden increase could result from some of the smallest particles being subthreshold and not counted until the Ca^{++} addition caused them to swell and possibly aggregate. No such increase in count was observed in curve 5 where a lower threshold was employed.

The effect of Ca^{++} addition on the length and volume distributions of myofibrils suspended in ATP solutions is shown in Figs. 6, 7, and 8. Fig. 6 illustrates the 200 channel volume histogram (A and C) and the 400 channel length histogram (B and D) as actually stored by the Didac. With the length distributions, contraction has steepened the right-hand slope so that it is above the control curve at lower channels and below the control curve at higher channels. With the volume distribution, contraction has elevated the flatter central portion of the curve and depressed the steeper left-hand region. In both length and volume histograms, a definite cross-over of the curves can be seen.

At the top of Figs. 7 and 8, the volume n_i (left) and length (right) are plotted in terms of the per cent of total count in each of 18–19 subgroups. At the bottom of Figs. 7 and 8, the volume shift Δn_i (left) and the length shift (right) are also plotted in terms of per cent of total count in the subgroups. The circles represent the shift occurring upon addition of ATP in the presence of EGTA, and the squares represent the shift occurring upon subsequent addition of excess Ca^{++}. The volume shift upon addition of Ca^{++} has an initial negative region, $-\Delta n_i$, followed by a positive region, $+\Delta n_i$; the length shift has a central positive peak at channel 120–140, a negative final region and a variable initial region. Fig. 7 represents a sample examined at room temperature in which considerable aggregation occurred upon addition of Ca^{++}. Fig. 8 was obtained from another sample examined at 0°C in which apparently no aggregation occurred upon addition of Ca^{++}. The most notable differences between them are the following: in addition to a decrease of long-length particles due to shortening, Fig. 7 has a decrease of short-length particles presumably due to clumping; instead of a rapid decline of the volume $+\Delta n_i$ with increasing channel number, Fig. 7 has a gradual decline extending beyond channel 199.

The volume distribution data relating to Fig. 8 are listed in Table I. A simple method of measuring an increase in volume is to compare the subgroups where a given per cent of count n_i is found, $i_{\text{after}}/i_{\text{before}}$. For example, a 50 % increase in volume would move n_4 to n_6, n_6 to n_9, n_8 to n_{12}, etc., since $6/4 = 9/6 = 12/8 =$

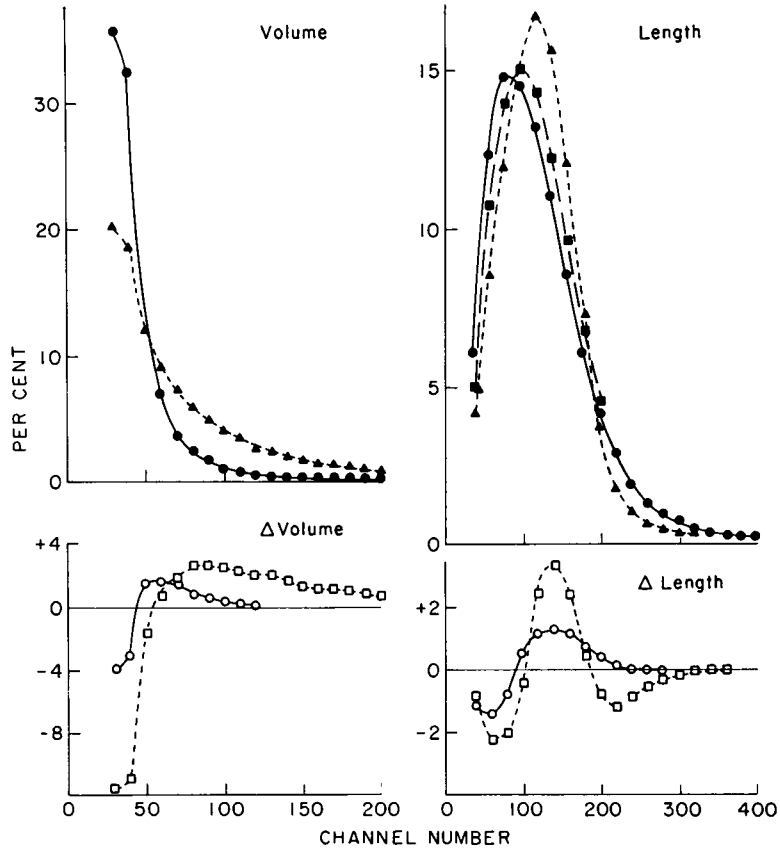

FIGURE 7 Response of myofibrillar effective volume and length to addition of ATP and then Ca^{++} at room temperature, with occurrence of aggregation. The 20 ml reaction mixture contained 2 mg myofibrils, 0.1 M KCl, 0.5 mM Mg^{++}, 0.5 mM creatine phosphate, 0.5 mg creatine kinase and 10^{-5} M EGTA in 0.02 M Tris-maleate buffer pH 6.85. The memory has been integrated in 18 subgroups of 10 channels (volume) or 19 subgroups of 20 channels (length). The count in each subgroup is expressed in terms of per cent of the total count. ●———●, control values for above reaction mixture. ■— — — — —■, values upon addition of 5×10^{-4} M ATP. ○———○, difference between values upon addition of 5×10^{-4} M ATP and control values. ▲- - - - -▲, values upon addition of 10^{-5} M Ca^{++}. □- - - - -□, difference between values upon addition of 10^{-5} M Ca^{++} and values in the presence of 5×10^{-4} M ATP. The total counts were: for the control, 161,000 volume and 189,000 length; after addition of ATP, 148,000 volume and 205,000 length; after addition of Ca^{++}, 131,000 volume and 158,000 length.

150%. In Table I it can be seen that the addition of Ca^{++} has moved n_8 to n_{10} and n_{12} to n_{15}, corresponding to a 25% increase in volume. Another method of measuring increase in volume which utilizes all of the data is to compare the total volume, $(\sum n_i V_i)_{\text{after}}/(\sum n_i V_i)_{\text{before}}$. In Table I this calculation indicates that there is about a 20% increase in volume upon addition of Ca^{++}.

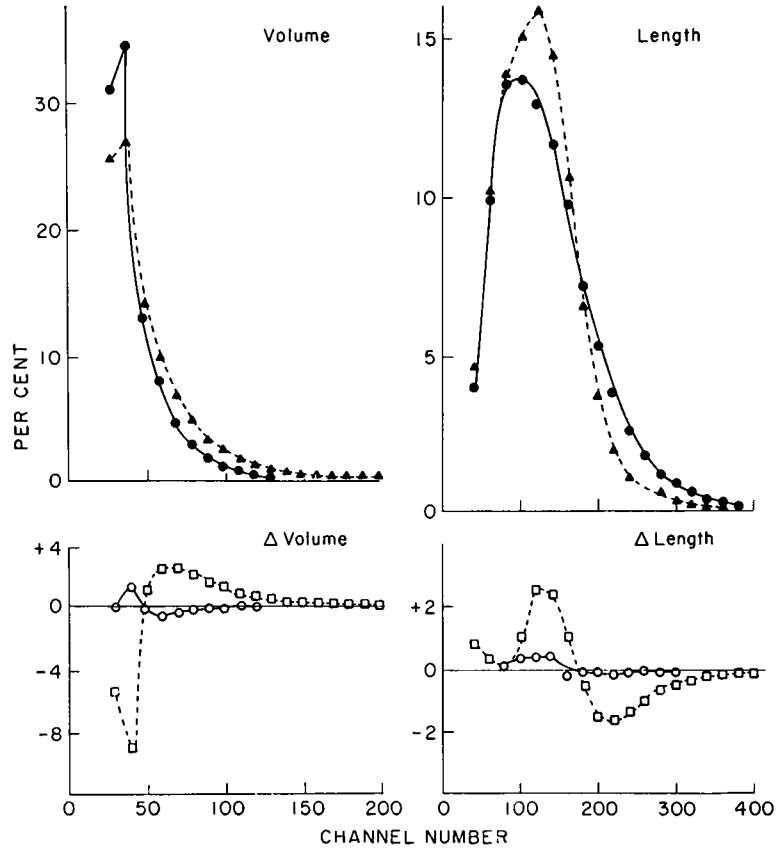

FIGURE 8 Response of myofibrillar effective volume and length to addition of ATP and then Ca^{++} at 0°C with freedom from aggregation. The 40 ml reaction mixture was as in Fig. 7. Symbols are as in Fig. 7, except that 2.5×10^{-4} M ATP and 5×10^{-6} M Ca^{++} were added. The total counts were: for the control, 113,000 volume and 138,000 length; after addition of ATP, 108,000 volume and 133,000 length; after addition of Ca^{++}, 138,000 volume and 171,000 length. For further details see text, Table I, and Fig. 5, curve 4.

As the final column in Table I illustrates, EGTA addition caused no reversal of the volume changes induced by Ca^{++}. It also had no effect on the length pattern. Similar negative results were routinely encountered. The myofibrils remained short and swollen, although EGTA had reduced the free Ca^{++} to very low levels. Because of the difference in pH between the turbidity experiments of Fig. 4 and the sizing experiments, the reversibility of turbidity development was tested in the pH 6.85 stock solution using creatine kinase as regenerating system; similar turbidity reversal to that of Fig. 4 C was obtained.

Since there remained the possibility that under the conditions of the sizing measurements irreversible turbidity development might be favored, conditions were sought for insuring turbidity reversibility. It was found that if myofibrils were

TABLE I

VOLUME DISTRIBUTION FOR THE MYOFIBRIL SAMPLE OF FIG. 8

		ATP absent		ATP present					
		Control		10^{-5} M EGTA		Same $+10^{-5}$ M Ca^{++}		Same $+10^{-4}$ M EGTA	
Count		113,000		108,000		138,000		125,000	
Channel	V_i	n_i	n_iV_i	n_i	n_iV_i	n_i	n_iV_i	n_i	n_iV_i
21–30	2	31.0	62.0	31.1	62.2	25.7	51.4	24.0	48.0
31–40	3	34.6	103.8	36.0	108.0	27.0	81.0	26.3	78.9
41–50	4	13.1	52.4	13.0	52.0	14.1	56.4	14.1	56.4
51–60	5	7.9	39.5	7.4	37.0	9.8	49.0	10.0	50.0
61–70	6	4.8	28.8	4.5	27.0	6.9	41.4	7.2	43.2
71–80	7	2.9	20.3	2.7	18.9	4.8	33.6	5.0	35.0
81–90	8	1.8	14.4	1.7	13.6	3.3	26.4	3.5	28.0
91–100	9	1.2	10.8	1.1	9.9	2.4	21.6	2.5	22.5
101–110	10	0.76	7.6	0.7	7.0	1.65	16.5	1.8	18.0
111–120	11	0.57	6.3	0.5	5.5	1.2	13.2	1.35	14.8
121–130	12	0.36	4.3	0.37	4.4	0.85	10.2	0.9	10.8
131–140	13	0.26	3.4	0.27	3.5	0.6	7.8	0.7	9.1
141–150	14	0.22	3.1	0.22	3.1	0.5	7.0	0.55	7.7
151–160	15	0.18	2.7	0.16	2.4	0.37	5.5	0.42	6.3
161–170	16	0.15	2.4	0.13	2.1	0.31	5.0	0.33	5.3
171–180	17	0.12	2.0	0.14	2.4	0.23	3.9	0.24	4.1
181–190	18	0.1	1.8	0.1	1.8	0.18	3.3	0.22	4.0
191–199	19	0.1	1.9	0.1	1.9	0.15	2.8	0.16	3.0
Total count $\sum n_i$		100.1		100.2		100.0		99.3	
Total volume $\sum_{i=2}^{i=19} n_iV_i$			367.5		362.7		436.0		445.1
Normalized			100.0		98.5		119.0		121.0

brought to pH 4.8 and held there for 10–20 min at 0–20°C, the aggregation encountered in Figs. 4 A and B no longer occurred. This is illustrated in Fig. 9. Even at room temperature in the presence of excess Ca^{++}, no aggregation occurred and the turbidity development was completely reversible. A series of sizing measurements was carried out on such pH 4.8-treated myofibril suspensions.

Fig. 10 indicates a direct proportionality between the volume shift obtained from difference curves as in Figs. 7 and 8 and the volume increase calculated as in Table I. It suggests that a 10% volume increase will be associated with a 6% volume shift.

Fig. 11 compares the length shift to the simultaneous volume shift of the same myofibril preparation. Although in a few cases as much as 16% length shift was found, most of the preparations underwent a 5–10% length shift. In pH 4.8-treated myofibrils this corresponded to a 4–8% volume shift (7–13% volume increase), while in untreated myofibrils this corresponded to a 7–25% volume shift (12–40% volume increase). The meaning of a 10% length shift could be that all myofibrils have shortened 10%, that half have shortened 20% and half have not shortened, etc. A

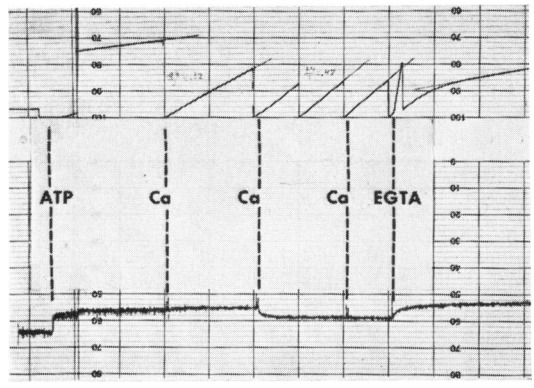

FIGURE 9 Response of ATPase activity and turbidity of pH 4.8-treated myofibrils to additions of Ca^{++}, and reversibility with EGTA. The 20 ml reaction mixture containing 6 mg myofibrils, 0.1 M KCl, and 0.5 mM Mg^{++} was brought to pH 4.7 in the pH stat, held there 24 min and returned to pH 7.3. At this time 0.5 mM acetyl phosphate, 0.05 mg *E. coli* acetokinase and 10^{-5} M EGTA were added. At the point labeled "ATP," the solution was brought to 10^{-3} M ATP; at the points labeled "Ca," 10^{-5} M Ca^{++} was added; and at the point labeled "EGTA," the solution was brought to 10^{-4} M EGTA. The time scale, turbidity scale, and ATPase scale are the same as in Fig. 4. The temperature was 22°C.

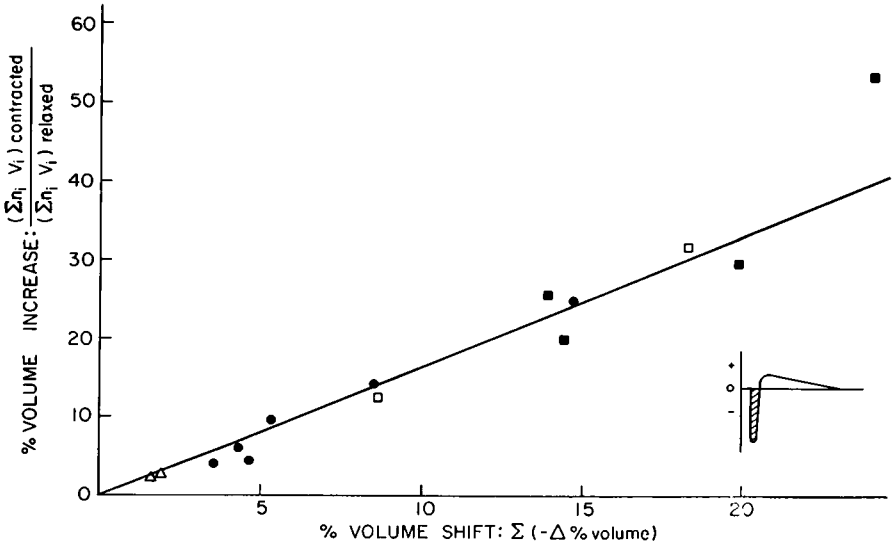

FIGURE 10 Relationship between the volume increase calculated as in Table I and the volume shift obtained as in Fig. 8. ●, pH 4.8-treated myofibrils, swelling occurred upon addition of Ca^{++}. ■, untreated myofibrils, swelling occurred upon addition of Ca^{++}. □, untreated myofibrils, swelling occurred upon addition of ATP. △, pH 4.8-treated myofibrils, reversal of swelling upon addition of EGTA.

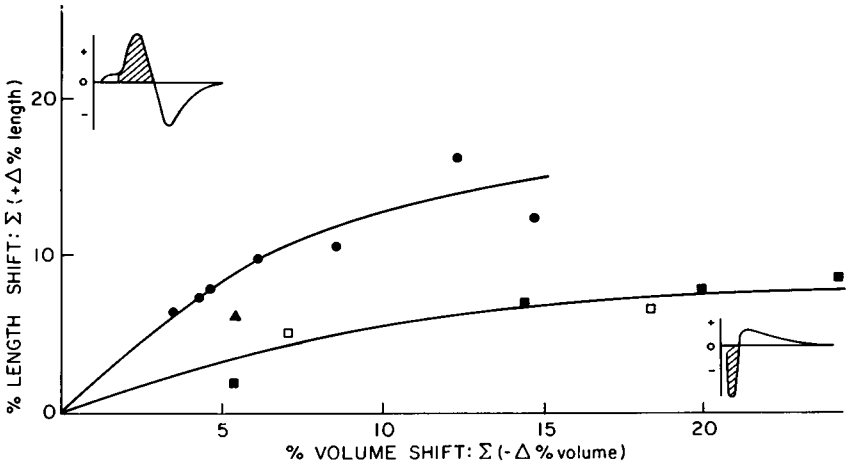

FIGURE 11 Relationship between the length shift and the volume shift obtained as in Fig. 8. ●, pH 4.8-treated myofibrils, contraction on addition of Ca^{++}. ■, untreated myofibrils, contraction on addition of Ca^{++}. □, untreated myofibrils, contraction on addition of ATP. ▲, myofibrils from rigor muscle, contraction on addition of Ca^{++}.

few measurements under phase microscopy indicated a sarcomere length of about 2.2 μ, suggesting that contraction below the 2.6 μ rest length had occurred in the course of preparation. With a 10% length shift, supercontraction must have occurred unless some of the myofibrils were initially at greater than 2.2 μ length.

At least part of the volume increase associated with shortening in the untreated myofibrils might be assigned to the irreversible aggregation which the fibers can undergo. No such explanation is possible for the pH 4.8-treated ones; their volume increase must be related to the shortening, since no aggregation occurs (Fig. 9).

Although the pH 4.8 treatment assured reversibility of turbidity development, no convincing reversal of length and volume changes was obtained upon addition of EGTA. Occasionally small reversals of volume and length changes have been encountered, especially in very fresh preparations (see Fig. 10, triangles). Conditions that will produce convincing and reproducible examples of reversibility are being actively pursued.

DISCUSSION

The increased protein effective volume observed experimentally upon addition of Ca^{++} to myofibrils was presumably due to incorporation into the domain of the protein of tightly bound water. This tightly bound water would have less conductivity than free water (27) and would offer increased viscous resistance to the passage of electrolyte ions. From direct measurement of crystal hydration (28) as well as from hydrodynamic calculations of protein swelling (28, 29), the presence of variable

amounts of tightly bound water in various protein molecules has been estimated. Such tightly bound water is an essential part of the muscle structure; the familiar denaturation of myosin by freezing is related to an irreversible loosening of bound water (30). Nuclear magnetic resonance studies reveal that muscle water is more structured than liquid water, and that a minor fraction has an extremely high degree of structure (31, 32).

The discussion of the preceding paragraph has been concerned with *volume transfer*, as defined in the introduction. Baskin studied volume changes of myofibrils inside a closed chamber (10); these were *volume variations*, as defined in the introduction. Since Baskin employed 5 mM potassium oxalate, his conditions would be comparable to those in the presence of EGTA where myofibril suspensions were turbid below about 2×10^{-5} M ATP and clear above this concentration (26). Baskin found that at 1.6×10^{-5} M ATP there was a volume decrease accompanying contraction of myofibrils, while at 6.4×10^{-5} M ATP there was a volume increase and no contraction (10). If Baskin's results may be compared and applied to the present ones, it appears that contraction of myofibrils concomitantly produces a drop in the volume of the system (*volume variation*) and a rise in the hydrated protein volume (*volume transfer*).

Both of these volume changes can be explained by the breaking of hydrophobic bonds within a protein such as myosin and the introduction of these hydrophobic groups into water. This would produce an immediate volume decrease (33, 34). Immobilization of water structure would also produce positive second virial coefficients analogous to those produced by charge effects in the case of osmotic pressure (35).[2] Similar to the effect of increasing charge, breaking hydrophobic bonds should cause increased osmotic pressure in membrane-limited systems or increased swelling of unbounded polymeric systems (37). In this way both the volume decrease found by Baskin and the swelling found in the present experiments could arise from a hydrophobic transition.

In smooth muscle cells, the cell membrane would enclose the system and an osmotic pressure could develop. Hill has measured an internal pressure in striated muscle, which he thought might arise from the straightening of curved fibers (38). Both electron microscopic (39) and X-ray studies (40) have revealed a lateral alignment of cross-bridges in muscle; swelling of such aligned cross-bridges would tend to spread apart the myosin lattice. The loss of intensity of the off-meridional layer lines attributed to the cross-bridges during muscle contraction (40, 41) could arise in part from disordering associated with the swelling process. Both internal pressure against the cell membrane and swelling apart of the myosin lattice would tend to increase the diameter of an elongated muscle cell. In a closed system an increase in diameter

[2] The proof of this statement has been submitted for publication elsewhere (44). Briefly it rests upon the relationship $B = (\varphi_2 - 1)/(c_2 M_2)$, where B is the second virial coefficient, c_2 is the concentration, M_2 the molecular weight and φ_2 the osmotic coefficient of hydrophobic amino acid residues as obtained experimentally (36).

would be accompanied by a decrease of length, and the process would be isovolumic (42). In an open system such as skinned fibers (43) or myofibril suspensions, lateral swelling of the myosin lattice would have to be accompanied by a longitudinal attractive force between actin and myosin filaments in order for tension or shortening to occur (44).

A serious question may be raised as to whether the present experiments are concerned with true contraction of myofibrils. Since the initial sarcomere length is approximately 2.2 μ, any shortening would have to be defined as supercontraction, and thus rather unphysiological. Failure of reversibility of length and volume changes could indeed be related to the occurrence of supercontraction rather than contraction. The fact of this irreversibility in conjunction with the clear-cut and reproducible reversibility of the ATPase activity and turbidity changes can be of great significance. It could signify the uncoupling in vitro of two processes which are ordinarily coupled in vivo. In the sense of Caplan's nonequilibrium thermodynamic analysis of muscle contraction (45), the input process would be ATP hydrolysis while the output process would be contraction. Reversibility of contraction has been reported in unloaded skinned fibers (46), in unloaded glycerol-extracted fiber bundles (47), and in fresh muscle homogenate (1). Partial reversal of size changes has been found in preliminary tests using the present procedures with fresh, briefly treated myofibrils.

Analogies have been drawn between turbidity development and contraction by many authors, after the original sample of Szent-Györgyi (48). What becomes of these analogies in the light of the present demonstration that turbidity development may be reversible under conditions where contraction of myofibrils is irreversible?

An answer rests upon defining the origin of the turbidity changes. Matsunaga and Noda demonstrated a direct relationship between turbidity and flow birefringence of actomysin suspensions at various ATP concentrations (49); Maruyama and Gergely had earlier shown that flow birefringence measures the degree of association between actin and myosin in these suspensions (50). An increased turbidity would be expected if the molecular weight were increased at constant protein concentration (and no variation occurred in the second virial coefficient). Thus association of actin with myosin can give increased turbidity, while dissociation results in clearing. It can be easily demonstrated that swollen suspensions of actomyosin or myofibrils at low ionic strength become more turbid as the ionic strength is raised and the swelling reduced. This could be predicted from the fact that raising the second virial coefficient diminishes the turbidity at finite concentration (if no variation occurs in the molecular weight). Thus swelling is a second source of clearing in myofibril suspensions.

The complex interplay possible between these two factors is suggested by Fig. 9. Although the first addition of Ca^{++} caused a marked increase in ATPase activity, no change in turbidity occurred. A possible explanation is that the increased turbidity accompanying actin association with myosin was masked by a concomitant decreased turbidity due to swelling. Only with further addition of Ca^{++} did further

actin-myosin association outweigh the swelling. In a parallel sample, contraction of myofibrils was found after the first addition of Ca^{++}; thus in this case it would appear misleading to assume that turbidity represents contraction. It must be added that such results are only rarely encountered; usually when Ca^{++} is added to cleared suspensions, increased ATPase activity is accompanied by increased turbidity as in Fig. 4.

Thus on two counts it appears to be unwarranted to equate turbidity development with contraction. Instead turbidity changes are related to inter- and intramolecular rearrangements of which the most significant involves the actin-myosin interaction (49, 50) while secondarily comes the state of swelling of the amorphous region of myosin (35). The actin-myosin interaction is reversible, judging by the reversibility of turbidity development under proper conditions, whereas the swelling and shortening have been found to be irreversible if supercontraction had developed. Thus part of the turbidity change—the actin-myosin binding—is related to the input process, while another part—the swelling—is related to the output process. Usually the input portion related to ATPase activity has been dominant and reversibility was found; occasionally the output portion masked it, as just discussed with Fig. 9, or when the unfolded hydrophobic groups interacted to produce aggregation as in untreated myofibrils.

It remains to be elucidated how the pH 4.8 treatment "vulcanized" the myofibrils so that aggregation could no longer occur. It is possible that previous myofibril preparations which manifested nicely reversible turbidity properties without such treatment (51) had not been buffered adequately to prevent the pH from dropping to near 5 in the course of preparation.

The author gratefully acknowledges the enthusiastic support of J. Haigh and E. Rapkin which made this work possible.
He also thanks M. Johnson for the fresh mouse and rat cells, and W. K. Engel for staining myofibril preparations.

Received for publication 8 May 1970 and in revised form 19 August 1970.

REFERENCES

1. MARSH, B. B. 1952. *Biochim. Biophys. Acta.* **9**:247.
2. WEBER, A. 1969. *J. Gen. Physiol.* **53**:780.
3. BRISKEY, E. J., K. SERAYDARIAN, and W. F. H. M. MOMMAERTS. 1967. *Biochim. Biophys. Acta.* **133**:412.
4. RAFF, E. C., and J. J. BLUM. 1966. *J. Cell Biol.* **31**:445.
5. LYNN, W. S. 1965. *Arch. Biochem. Biophys.* **110**:262.
6. ERNST, E. 1925. *Pfluegers Arch. Gesamte Physiol. Menschen Tiere.* **209**:613.
7. ERNST, E. 1963. Biophysics of the Striated Muscle. Akademiai Kiado, Budapest. 187,340.
8. MEYERHOF, O., and W. MOHLE. 1935. *Pfluegers Arch. Gesamte Physiol. Menschen Tiere.* **236**:533.
9. ABBOTT, B. C., and R. J. BASKIN. 1962. *J. Physiol. (London).* **161**:379.
10. BASKIN, R. J. 1964. *Biochim. Biophys. Acta.* **88**:517.
11. HOTTA, K., and F. TERAI. 1966. *Arch. Biochem. Biophys.* **114**:288.
12. BASKIN, R. J., and P. J. PAOLINI. 1966. *J. Gen. Physiol.* **49**:387.

13. BASKIN, R. J., and P. J. PAOLINI. 1967. *Amer. J. Physiol.* **213**:1025.
14. CATTELL, M., and D. J. EDWARDS. 1928. *Amer. J. Physiol.* **86**:37.
15. EBBECKE, U., and O. HASENBRING. 1935. *Pfluegers Arch. Gesamte Physiol. Menschen Tiere.* **236**:405.
16. MARSLAND, D. A., and D. E. S. BROWN. 1942. *J. Cell. Comp. Physiol.* **20**:295.
17. RAINFORD, P., H. NOGUCHI, and M. MORALES. 1965. *Biochemistry.* **4**:1958.
18. IKKAI, T., and T. OOI. 1969. *Biochemistry.* **8**:2615.
19. MATTERN, C. F. T., F. S. BRACKETT, and B. J. OLSON. 1957. *J. Appl. Physiol.* **10**:56.
20. BULL, B. S. 1968. *Blood J. Hematol.* **31**:503.
21. IZAWA, S., M. ITOH, and K. SHIBATA. 1963. *Biochim. Biophys. Acta.* **75**:349.
22. GEBICKI, J. M., and F. E. HUNTER, JR. 1964. *J. Biol. Chem.* **239**:631.
23. KUBITSCHEK, H. E. 1968. *Biophys. J.* **8**:792.
24. GROVER, N. B., J. NAAMAN, S. BEN-SASSON, F. DOLJANSKI, and E. NADAV. 1969. *Biophys. J.* **9**:1398.
25. EVANS, T. C., and W. J. BOWEN. 1968. *Anal. Biochem.* **25**:136.
26. KOMINZ, D. R. 1970. *Biochemistry.* **9**:1792.
27. JACCARD, C. 1965. *Ann. N. Y. Acad. Sci.* **125**:390.
28. COHN, E. J., and J. T. EDSALL. 1943. Proteins, Amino Acids and Peptides. Reinhold Publishing Corp., New York, Chap. 16.
29. SCHERAGA, H. A., and L. MANDELKERN. 1953. *J. Amer. Chem. Soc.* **75**:179.
30. LOVE, R. M., and M. K. ELERIAN. 1963. *Proc. Int. Congr. Refrig. 11th.* 887.
31. COPE, F. W. 1969. *Biophys. J.* **9**:303.
32. HAZLEWOOD, C. F., B. L. NICHOLS, and N. F. CHAMBERLAIN. 1969. *Nature (London).* **222**:747.
33. NEMETHY, G., and H. A. SCHERAGA. 1962. *J. Chem. Phys.* **36**:3401.
34. NEMETHY, G., and H. A. SCHERAGA. 1962. *J. Phys. Chem.* **66**:1773.
35. KOMINZ, D. R. 1968. *In* Symposium on Muscle, E. Ernst and F. B. Straub, editors. Akademiai Kiado, Budapest. 109.
36. SMITH, P. K., and E. R. B. SMITH. 1937. *J. Biol. Chem.* **121**:607.
37. KUHN, W., A. RAMEL, and D. H. WALTERS. 1960. *In* Size and Shape Changes of Contractile Polymers. A. Wasserman, editor. Pergamon Press, Inc., New York. 41.
38. HILL, A. V. 1948. *J. Physiol. (London).* **107**:518.
39. PEPE, F. A. 1967. *J. Mol. Biol.* **27**:203.
40. HUXLEY, H. E., and W. BROWN. 1967. *J. Mol. Biol.* **30**:383.
41. TREGEAR, R. T., and A. MILLER. 1969. *Nature (London).* **222**:1184.
42. ELLIOTT, G. F., J. LOWY, and B. M. MILLMAN. 1967. *J. Mol. Biol.* **25**:31.
43. HELLAM, D. C., and R. J. PODOLSKY. 1969. *J. Physiol. (London).* **200**:807.
44. KOMINZ, D. R. 1970. *J. Theor. Biol.* In press.
45. CAPLAN, S. R. 1968. *Biophys. J.* **8**:1146, 1167.
46. PODOLSKY, R. J., and L. L. COSTANTIN. 1964. *Fed. Proc.* **23**:933.
47. RANNEY, R. E. 1954. *Amer. J. Physiol.* **179**:99.
48. SZENT-GYÖRGYI, A. 1947. Chemistry of Muscular Contraction. Academic Press, Inc., New York. 31.
49. MATSUNAGA, T., and H. NODA. 1966. *J. Biochem. (Tokyo).* **60**:674.
50. MARUYAMA, K., and J. GERGELY. 1962. *J. Biol. Chem.* **237**:1095, 1100.
51. MARUYAMA, K., and D. R. KOMINZ. 1967. *J. Biochem. (Tokyo).* **65**:465.